Nature and evolution of metamorphic fluids associated with turbidite-hosted gold deposits: Hill End goldfield, NSW, Australia

P. K. SECCOMBE AND J. LU

Department of Geology, The University of Newcastle, Callaghan NSW 2308, Australia

AND

A. S. ANDREW, B. L. GULSON AND K. J. MIZON

Division of Exploration Geoscience, CSIRO, PO Box 136, North Ryde, NSW 2113, Australia

Abstract

The Hill goldfield, NSW, Australia, is an example of a syntectonic, slate-belt gold deposit formed in a multiply deformed, Late Silurian slate-metagreywacke turbidite sequence. Gold is confined to bedding-parallel veins and discordant leader veins composed of as many as four generations of quartz, accompanied by phyllosilicates, carbonates and minor sulphides. Vein formation and gold deposition was apparently synchronous with Early Carboniferous metamorphism and deformation. Homogenisation temperatures (T_h) for fluid inclusions in vein quartz demonstrate five groupings in the temperature intervals 350–280 °C, 280–250 °C, 250–190 °C 190–150 °C, and 150–110 °C, corresponding to a variety of primary and secondary inclusions developed during four periods of vein quartz deposition under a generally declining temperature regime. Inclusion fluids are characterised by a low salinity of around 0.1 to 3.6 wt.% NaCl equivalent. The dominant gas phase present in the inclusion fluids varies from N_2 in the early stages of the paragenesis, through CH_4 during the main episode of gold deposition, to CO_2-rich fluids associated with late-stage mineralisation. $\delta^{18}O$ values for vein quartz (range 15.1–17.1‰) and vein carbonate (range 11.3–13.4‰) are typical of metamorphic mineralisation. δD composition of hydrous minerals and inclusion fluids (range −53 to −138‰) suggest an influx of meteoric water in the later mineralising fluids. This conclusion is supported by $\delta^{13}C$ data for vein calcite (range −2.5 to −9.7‰). $\delta^{34}S$ composition of vein pyrrhotite and pyrite ranges from 6.9 to 7.8‰ early in the paragenesis, to lighter values (around 4.2 to 5.8‰) accompanying late gold deposition from more oxidising fluids. Sulphur isotope data imply a sulphur source from underlying turbidites and an increase in fluid oxidation state during mineralisation. Lead isotope measurements on vein pyrite, arsenopyrite, galena and gold are characterised by two isotope populations with $^{207}Pb/^{206}Pb$ ratios of 0.862 and 0.860, which define two discrete mineralising events during vein formation. Consistency between data from vein minerals and lead isotope signatures for potential source rocks indicate that lead was derived from the sedimentary pile.

KEYWORDS: fluid inclusions, stable isotopes, lead isotopes, gold, metamorphic fluids, Australia.

Introduction

STUDIES of a wide variety of vein gold deposits in low- to medium-grade metamorphic environments point to the important role that metamorphic fluids play in mobilising gold from crustal rocks and precipitation of the metal in structurally focussed sites during deformation events. Modelling of fluid compositions derived from metamorphic dehydration reactions accompanying amphibolite facies metamorphism of crustal rocks (Powell *et al.*, 1991) and fluid inclusion studies of mesothermal gold deposits in metamorphosed volcano–sedimentary settings (Ho, 1987) highlight the reduced, low salinity, high CO_2 content of the fluids involved in transporting gold in the mesothermal environment. In turbidite successions, structural investigations on auriferous quartz veins indicate that vein formation may extend over the entire deformation episode (Cox,

Mineralogical Magazine, September 1993, Vol. 57, pp. 423–436

et al., 1991) and that individual veins commonly develop from a 'crack-seal' (Ramsay, 1980) process involving incremental addition of vein laminae.

Although the composition of the mineralising fluids in metamorphic environments are moderately well established and timing relationships of gold precipitation relative to the metamorphic peak can be deduced, few studies have attempted to document the evolution of the mineralising system throughout the metamorphic event. In this paper, we present the results of a mineralogical and textural study of a turbidite-hosted gold vein deposit which allows five stages of fluid activity to be distinguished during the construction of individual gold-bearing veins. Definiton of these episodes of mineralisation is important for the interpretation of isotope and fluid inclusion data and in developing a model of fluid evolution during deposition of the veins. In this way, we can demonstrate an early period of mineralisation, corresponding to two stages of deposition of barren quartz, followed by three periods of gold deposition, all accompanied by a progressive rise in the oxidation state of the ore-forming fluids. Each mineralising event may be defined by a particular ore and gangue mineral paragenesis and particular geochemical criteria, all of which place important constraints on the source of gold, fluids and other vein components. The results also provide significant exploration implications concerning the movement of gold in slate belts.

General geology

Gold-bearing quartz veins are developed within a thick sequence of pelites and quartz-rich and tuffaceous arenites of turbidite origin, which represent the oldest trough-fill units of a post-Mid Silurian pull-apart basin, formed between two segments of an older Palaeozoic andesitic, volcanic arc in the Lachlan Fold Belt of south-eastern Australia. Richest gold veins developed close to the hinge of the doubly plunging Hill End Anticline (Fig. 1), a regionally extensive F2 structure which controls similar vein-style mineralisation at Hargraves, 30 km to the N of Hill End. Rocks in the vicinity of Hill End have experienced biotite grade, greenschist facies regional metamorphism (Offler and Prendergast, 1985). Peak metamorphic *P/T* conditions of 2.9 kbar and 420 °C were estimated by Seccombe and Hicks (1989) from the silica content of white mica and the composition of coexisting syntectonic carbonates in the wallrocks. Usage of the prefix 'meta-' is implicit in the rock terms in this paper.

The timing of the major deformation affecting the central parts of the Hill End Trough is not well established. Conclusions extrapolated from studies on the E margin of the trough (Powell *et al.*, 1976; Powell and Edgecombe, 1978) suggest that the principal deformation (D2) and cleavage-forming event occurred during Early Carboniferous time. At Hill End, regional folds (F2) display northerly trends and upright axial surfaces (Figs. 1 and 2) and appear to relate to D2 deformation. A well developped axial plane cleavage (S2) strikes 170° and dips 80° E in the mine area. Two other cleavages are recognised in the area. A weak sub-vertical foliation which trends 115° and predates S2 is defined in the mine area (Hicks, 1977). This early foliation may be associated with a probable Middle Devonian E–W folding event recognised by Collins (1971). A crenulation cleavage (S3) which overprints the S2 slaty cleavage is variably developed in pelites (Hicks, 1977) and may relate to late kinematic kinking associated with the D2 deformation.

The most productive veins are encountered in the E-dipping limb of the anticline. Here, bedding-parallel veins, which range in thickness from 5 cm to several metres are observed in slate, close to contacts with graded greywacke units (Fig. 2). Individual veins persist along strike for several hundred metres and may be correlated with surface exposures in the shallow N-plunging hinge zone of the anticline or with veins intersected on the W-dipping limb. Production from the vein systems during the period 1865 to 1918 accounted for nearly 12.4 t of gold (Stevens, 1974).

Vein structure and mineralogy

The majority of the veins are laminated and appear to have formed by the incremental addition of material parallel to the vein walls, whereby laminae are added internally to the vein or screens of wallrock are incorporated in the vein due to rupture close to vein contacts. The following features described by Seccombe and Hicks (1989) and Windh (1993, in press) suggest that vein emplacement was probably initiated by flexural slip associated with the development of the Hill End Anticline and spanned the entire D2 deformation event:

1. Close to the anticlinal hinge, where bedding dips at shallow angles, vein thicknesses may reach 2m and folding of veins is common (Fig. 2). In this region, veins that have a thickness greater than 5 cm show open folds, whereas veins that are only a few mm thick are folded ptygmatically.

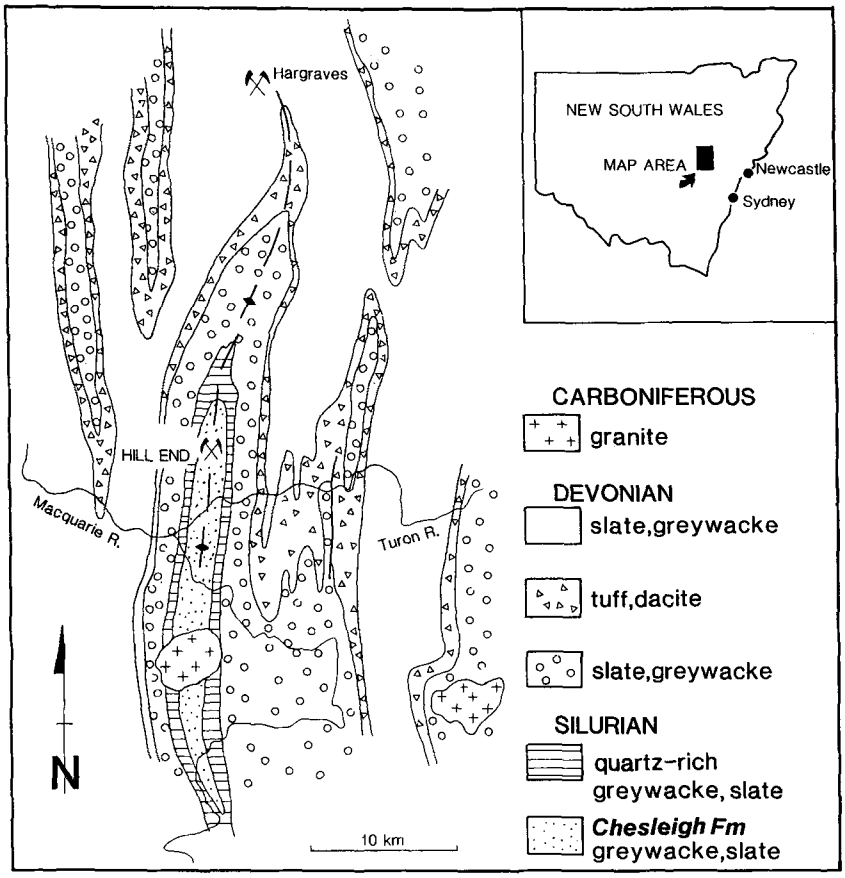

FIG. 1. Location and geological map of the Hill End goldfield, New South Wales.

Away from the fold hinge, bedding-parallel veins are thinner on the more steeply dipping fold limbs and are rarely folded; instead boudins are developed due to vein extension (Fig. 3a).

2. The orientation of axial surfaces to minor folds developed in the veins, boudin axes, and slickenlines developed on chloritic slate at vein contacts are all consistent with the regional fold geometry and their generation during the D2 deformation event.

3. Rare fragments of cleaved wallrock displaying S2 foliation are preserved within the laminated veins.

4. Growth fibres in vein quartz oriented nearly parallel to the vein walls, and cleavage reorientation in wallrocks adjacent to some steeply E-dipping veins, suggest that the veins acted as reverse faults late in their formation and opened under shear.

5. Intragranular deformation structures, involving the development of undulose extinction, deformation bands and deformation lamellae are confined to early generations of vein quartz and indicate that these developed prior to the last stages of regional deformation. Recovery and recrystallisation textures are characteristic of this early quartz.

6. Minor undeformed veins, oriented at a high angle to cleavage, developed late in the deformation event.

7. Small-scale faults, known as 'cross-courses' are gold-bearing and offset the veins in the underground workings by as much as 80 cm. Narrow (4–50 mm) quartz veins, referred to as 'leaders' (Fig. 3b) have a similar orientation to the faults and appear in the structural hangingwall of productive veins such as the Star of Hope and Mica veins (Fig. 2). The leaders intersect, but do not offset the major veins and are variably deformed. Leaders carry high gold values but are volumetrically insignificant in comparison with the principal bedding-parallel veins.

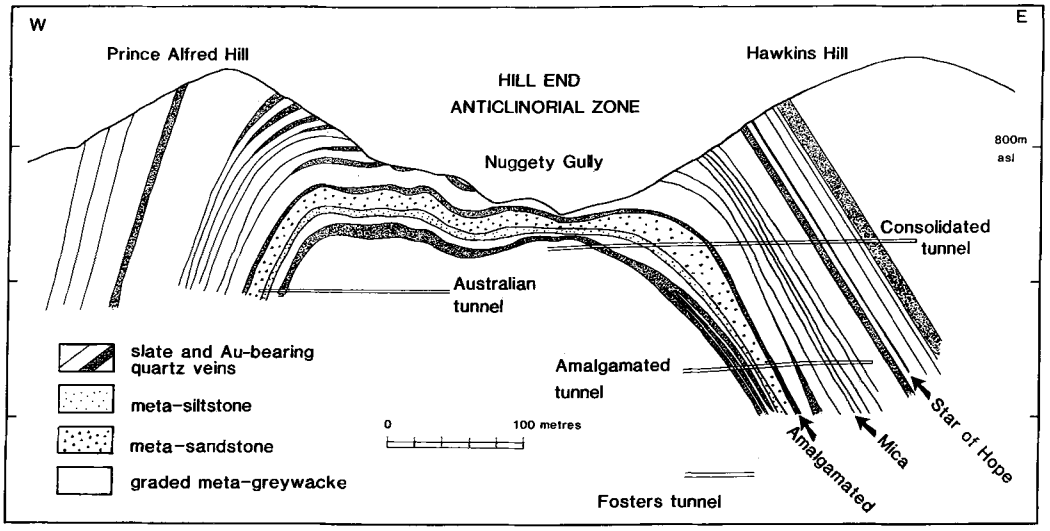

FIG. 2. Geological cross-section through the central part of the goldfield in the hinge of the Hill End Anticline. The section depicts the position of slate units (each generally contains an auriferous quartz vein), the projected location of accessible tunnels and named veins discussed in the text.

Both types of veins (bedding-parallel veins and leaders) are composed chiefly of quartz, carbonates and muscovite (sericite) with minor pyrrhotite and rare gold, pyrite, chalcopyrite, marcasite, sphalerite and galena. Resolution of multiple populations of ore and gangue minerals indicate that vein formation and accompanying gold mineralisation are the products of multi-stage fluid activity. Based on microstructural observations and overprinting relationships, five major periods of mineralisation are established for vein formation at Hill End (Fig. 4). Most vein minerals have been precipitated in at least two and as many as four paragenetic stages (Figs. 4 and 5*a*). The complete paragenesis appears consistently in the major auriferous bedding-parallel veins and associated auriferous leaders.

Gold and sulphide mineralisation postdates the two major stages of quartz accumulation in the veins (stage I and II quartz). In auriferous bedding-parallel and leader viens, gold is associated with muscovite, chlorite, calcite and sulphides (Fig. 5*b*). Whether it is distributed in microveinlets which are parallel to the earlier vein laminations in either vein type or in later, oblique veinlets, textural relationships always indicate that gold follows the first two stages of quartz deposition. At least three episodes of gold mineralisation have been identified (Fig. 4). A fuller description of the vein paragenesis and mineralogy is provided by Lu and Seccombe (1993, in press).

Fluid inclusion data

Based on the paragenetic stages defined above, constraints provided by fluid inclusions on the composition of the ore-forming fluids and the nature of the mineralising environment are critical in establishing the evolution of the vein system. The results of a major fluid inclusion study of the vein systems at Hill End, presented in Lu and Seccombe (1993, in press) are summarised here.

Fluid inclusions in quartz, either from bedding-parallel veins or from leader veins indicate a similar range in homogenisation temperature (T_h) from 350° to 110 °C (Figs. 6a to 6c). Within this range, the data demonstrate five groupings in the temperature intervals 350–280 °C, 280–250 °C, 250–190 °C, 190–150 °C and 150–110 °C, indicating that the two styles of veins were formed during similar events and are the products of the same episodes of fluid activity.

T_h of primary inclusions (Fig. 5*c*) identified in the first generation of quatz (stage I quartz) in the bedding-parallel veins and gold-bearing leader veins ranges from 350 °C to 280 °C which is lower than peak metamorphic temperatures in the study area. Evidence of re-equilibration of this population of inclusion under conditions of internal underpressure (Sterner and Bodnar, 1989) is consistent with fluid trapping and the precipitation of stage I quartz in the bedding-parallel veins prior to the attainment of peak metamorphic *P/T*

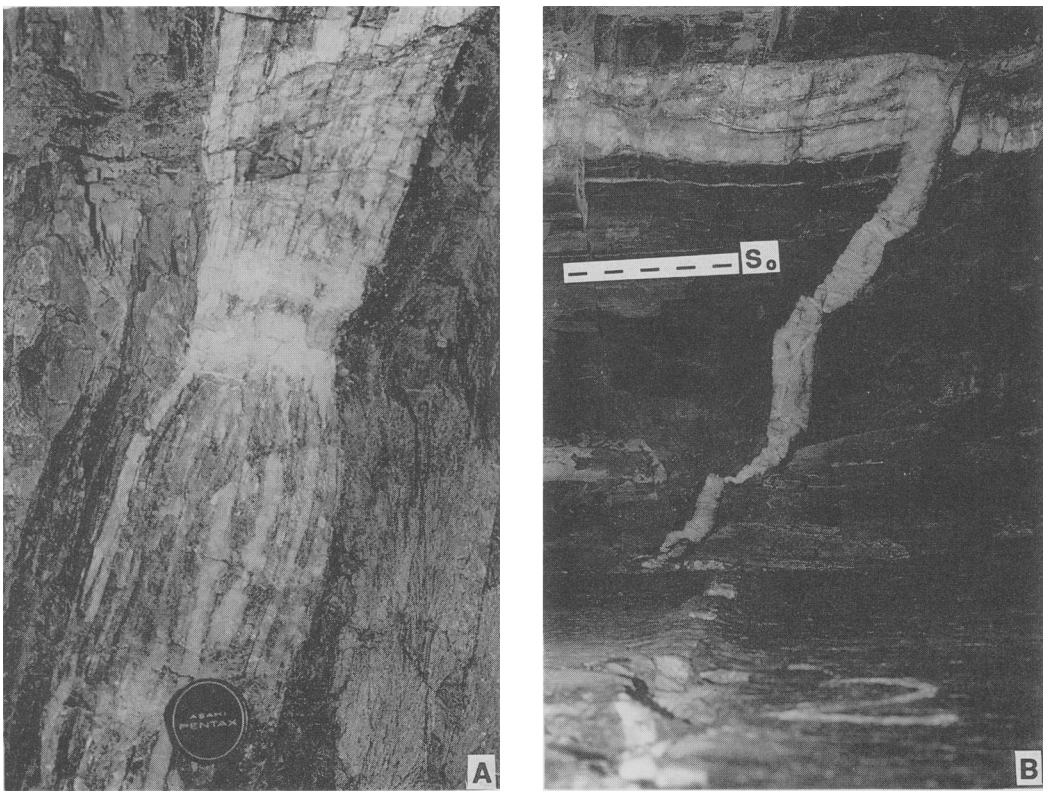

FIG. 3. Mesoscopic vein structures. A. Extended, steep W-dipping, laminated bedding-parallel vein developed in the pelitic top of a graded greywacke bed. Stage V quartz fills the boudin neck. N-wall, Australian tunnel. The scale is 5 cm in diameter. B. Plan view of the intersection, on the roof of an underground opening, of a deformed, 10 cm-wide leader vein with a 25 cm-wide, laminated bedding-parallel vein. Steep N-dipping leaders are encountered in the hangingwall of the major veins. The trace of bedding (S_0) and cleavage are nearly parallel. East vein, Consolidated tunnel.

conditions. Because of the effects of inclusion re-equilibration, the T_h data for inclusions trapped during this first episode of fluid activity represent minimum fluid temperatures for the mineralising fluids (op. cit.). However, the true fluid temperature may not have been much higher than the T_h range, because mineral assemblages from the veins and wallrock suggest that maximum temperatures did not exceed 420 °C.

Three groups of secondary fluid inclusions have been identified in stage I quartz. Group A secondary inclusion are confined to sealed cracks parallel to the laminations of the principal (bedding-parallel) quartz veins (Fig. 5*d*) and define two T_h ranges (280–250 °C and 250–190 °C). Some Group A secondary inclusions also appear to have experienced re-equilibration. Group B inclusions are confined to sealed cracks oblique to the vein laminations and are characterised by low T_h (150–190 °C).

Fluid inclusions are poorly developed in stage II quartz. T_h for primary inclusions in stage II quartz ranges from 250° to 280 °C. Secondary inclusions in stage II quartz display a T_h range from 240–190 °C and 190–150 °C.

Fluid inclusions are undeveloped in the stage III quartz. By contrast, in stage V quartz, well devloped inclusions are characterised by a wide variation in size, gas ratio, the presence of liquid CO_2 in some inclusions and T_h in the range 210–140 °C. Inclusion fluids from all generations of quartz typically have a low salinity of around 0.1–3.6 wt percent NaCl equivalent.

Laser Raman microprobe anlaysis indicates that the gas composition of the fluid inclusions relates to the paragenetic position of the host quartz. In stage I quartz, $H_2O(g)$ and N_2 dominate in the primary inclusions, CH_4 and CH_4 + $H_2O(g)$ are the principal species present in Group A and Group B secondary inclusions,but $H_2O(g)$

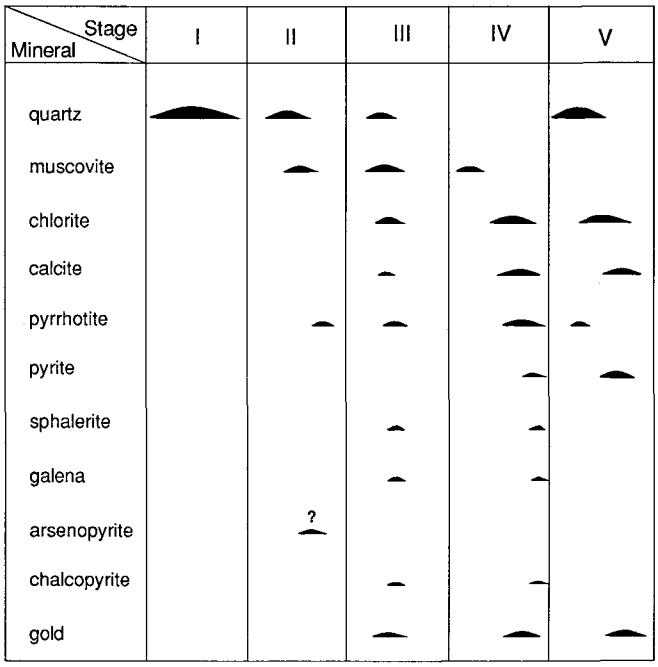

FIG. 4. Paragenetic diagram for stages of mineral deposition on the Hill End goldfield.

is the only major phase in group C secondary inclusions. In stage II quartz the gas phase composition is dominated by CH_4 and CH_4 + $H_2O(g)$. Gas phase composition in stage V quartz varies both with depth in the vein system and also from the earlier to late stages of stage V quartz deposition. Early in stage V, associated with the development of conformable and discordant chlorite and calcite veins in the footwall of the major bedding-parallel veins, quartz contains fluid inclusions characterised by $H_2O(g)$ and CH_4 + $H_2O(g)$. Inclusions associated with the deposition of late, stage V quartz and calcite in the crest of the major anticline, have CO_2 as the dominant gas phase, reflecting a change towards more oxidising conditions in the fluid during the final period of mineralisation. T_h data, low salinity, and variable amounts of N_2, CH_4 and CO_2 as gas species in a dominantly aqueous fluid are all consistent with a metamorphic derivation for the mineralising fluids (Kerrich, 1986; Goldfarb *et al.*, 1988). True trapping temperatures are difficult to estimate from the T_h data because of the problems in quantifying the temperature correction resulting from the combined effects of fluid pressure and variable fluid compositon for each episode of fluid activity (e.g., Bowers and Helgeson, 1983; Roedder, 1984). This is made more difficult in the metamorphic environment because of the likelihood of changes in fluid pressure in the vein system, resulting from possible tectonic thickening or erosion accompanying deformation.

However, an independent check on mineralising temperatures and the extent of the temperature corrections to fluid inclusion T_h data can be achieved using the geothermometer based on the composition of chlorite (Walshe, 1986). Depositional temperatures ranging from 296 to 270 °C are calculated from the composition of chlorite associated with gold deposition during paragenetic stages III to V, and imply that temperature corrections to some T_h data from stage V (T_h range 210–140 °C) may be as high as 120 °C (Lu *et al.*, 1993, in press).

Stable isotope geochemistry

Minerals prepared for isotope analysis included quartz (O-isotopes and H-isotopic composition of inclusion fluids) calcite (O- and C-isotopes), chlorite, muscovite, and biotite (O- and H-isotopes) and pyrrhotite and pyrite (S-isotopes).

Samples were prepared according to the following established methods: δD in water (Bigeleisen *et al.*, 1952), $\delta^{13}C$ and $\delta^{18}O$ in carbonates (McCrea, 1950), $\delta^{18}O$ in silicates (Clayton and Mayeda, 1963) and $\delta^{34}S$ (Robinson and Kusak-

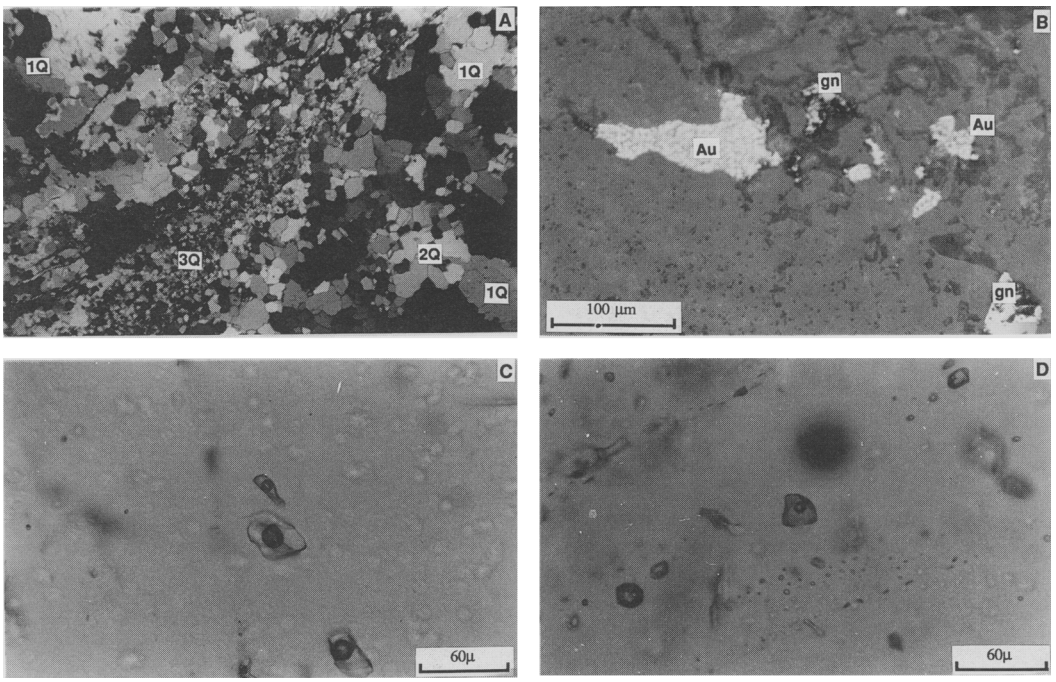

FIG. 5. Mineralogy and fluid inclusion petrography. **A.** Equant fine-grained stage III quartz (3Q) and medium-grained stage II quartz (2Q) define microveinlets developed in a bedding-parallel vein, parallel to vein laminations in strained stage I quartz (1Q). **B.** Disseminated gold (Au) and galena (gn) in quartz from a leader vein. **C.** N_2-bearing primary fluid inclusion in stage I quarz from a bedding-parallel vein. **D.** Planes of CH_4-bearing aqueous secondary fluid inclusion (Type 2A) in stage I quartz from a bedding-parallel vein.

abe, 1975). Isotope analyses were undertaken on MICROMASS 602 mass spectrometers located at the Division of Exploration Geoscience, CSIRO, North Ryde as part of the cooperative Centre for Isotope Studies. Results are presented in Figs. 7–9 as $\delta^{18}O$, δD, $\delta^{13}C$ and $\delta^{34}S$ values, relative to the V_{SMOW} standard for O- and H-isotopes, the PDB standard for C-isotopes and Canõn Diablo troilite for S-isotopes. Routine precision of the results are ±0.1‰ for $\delta^{34}S$ measurements on sulphides, $\delta^{13}C$ and $\delta^{18}O$ obtained from carbonates, ±0.2‰ for $\delta^{18}O$ from silicates, and ±2‰ for δD.

Results. $\delta^{18}O$ values for all samples of quartz are grouped in a relatively narrow range between 15 and 17‰. There appears to be no obvious variation among the different generations of quartz.

With one exception, $\delta^{18}O$ composition of calcite from the bedding-parallel veins ranges between 11.7 and 13.4‰. $\delta^{18}O$ values for the stage IV and V calcite from bedding-parallel veins and calcite from late-stage, barren carbonate-quartz veins in the wallrocks are distributed generally in the same range (11.3–12.6‰). However, the $\delta^{18}O$ ratio (9.2 and 19.7‰) for two calcite samples from late-stage veins apparently unrelated to gold mineralisation, lie well beyond this range.

Chlorite, generally representing paragenetic stages IV and V, gives a $\delta^{18}O$ distribution restricted to the range 8.4–11.0‰; similar to the value obtained for late-stage muscovite (11.0‰). Three samples of wallrock biotite are among the most depleted in $\delta^{18}O$, with values ranging from 5.5 to 9.1‰.

δD composition (nine samples; range −79 to −138‰) appears to decrease from muscovite (−83‰) through chlorite (−79 to −99‰), to biotite (−135, −138‰), consistent with the experimental results of Suzuoki and Epstein (1976) which demonstrate that D/H fractionation among silicates is mainly a function of the magnesium, aluminium and iron contents of the minerals. δD values obtained from the water released from fluid inclusions in samples of quartz (seven samples; range −53 to −77‰) give slight differences for different sample heating intervals. These differences are within 10‰ and are taken to indicate a consistency of isotopic composition

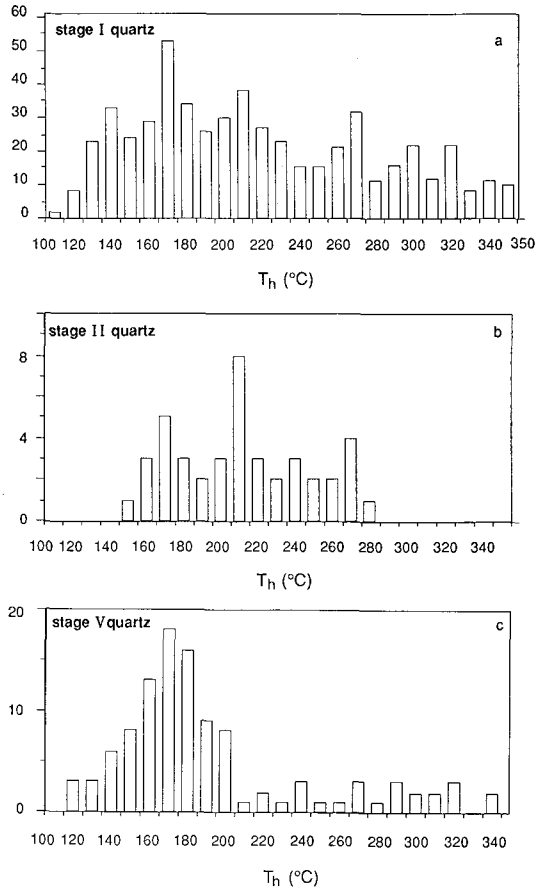

FIG. 6. Fluid inclusion geothermometry of Hill End quartz veins. **a.** T_h data for multiple fluid inclusion populations from stage I quartz. **b.** T_h data for stage II quartz. **c.** T_h data for stage V quartz from auriferous veins in the crest of the Hill End Anticline.

among the different generations of inclusions in each sample. A significant depletion in D/H ratio is encountered for stage V quartz deposition (average $\delta D = -73‰$) compared to earlier generations of quartz (stages I–III: average $\delta D = -56‰$).

C-isotopic composition of the calcite from the bedding-parallel veins ranges from −4.6 to −9.7‰, and that of the samples from the barren carbonate veins ranges from −2.5 to −6.7‰. For a temperature of 300 °C, the relevant value for the $\delta^{13}C_{H_2CO_3(ap)}$ of the fluid in equilibrium with stage IV calcite from the bedding-parallel veins ranges from −2.5 to −7.6‰, and that for the calcite in the barren, late-stage carbonate veins occupies the range from −0.4 to −4.7‰.

$\delta^{34}S$ values for pyrrhotite from the laminated veins, with only one exception (4.9‰), define a narrow range from 6.9 to 7.8‰. One pyrite from the bedding-parallel veins has a $\delta^{34}S$ value of 5.8‰.

$\delta^{34}S$ composition of disseminated pyrrhotite in greywacke and slate is restricted to a very narrow range from 4.3 to 5.0‰. By contrast, sulphide joint coatings in the wallrocks and disseminated pyrite in greywacke give a wide range in sulphur isotope distribution, ranging from −7.1 to 14.4‰. In the barren, late-stage quartz-carbonate veins, apart from one pyrite sample with a very unusual $\delta^{34}S$ value of 22.9‰, the range in isotopic composition lies between −8.5 and 6.5‰.

Stable isotope interpretation. An estimate of the bulk isotopic composition of the ore-forming fluid may be gained from the isotopic data to help define the source of fluids and vein components and the evolution of the mineralising system. For O− and H-isotope data, if we assume that equilibrium was achieved between minerals and the precipitating fluid, the corresponding $\delta^{18}O$ and δD values of the fluid can be calculated using established mineral–water fractionation factors (O'Neil and Taylor, 1969; Clayton *et al.*, 1972; Sakai and Tsutsumi, 1978). For a temperature of 300 °C, the $\delta^{18}O$ composition of the fluid in equilibrium with the early generations of quartz is calculated to have ranged from 8.2–10.2‰. Using the corresponding δD values available from extracted inclusion fluids, the data are located in the region defined by Taylor (1979) for the $\delta^{18}O$ and δD composition of metamorphic water.

By comparison, the O- and H-isotope composition, interpreted for quartz collected from stage V quartz–chlorite aggregates and massive quartz in the hinge of the anticline cannot be attributed solely to metamorphic water. Whereas the $\delta^{18}O$ values remain in a relatively narrow range, D/H ratios are depleted towards the later periods of stage V quartz deposition, signalling the likely entry of meteoric water into the mineralising system.

Irrespective of the paragenetic position, isotopic data from all analysed samples of chlorite are located in the metamorphic water area. The calculated $\delta^{18}O$ composition of fluid in equilibrium with biotite in the greywacke wallrock ranges from 9.0 to 12.6‰, within the range defined for a metamorphic fluid. However, the calculated δD values are extremely low, ranging between −85 and −88‰; well below the field for metamorphic water. The reason for this depletion is not clear and is the subject of further investigation.

Where present, calcite precipitates typically towards the later stages of each episode of fluid

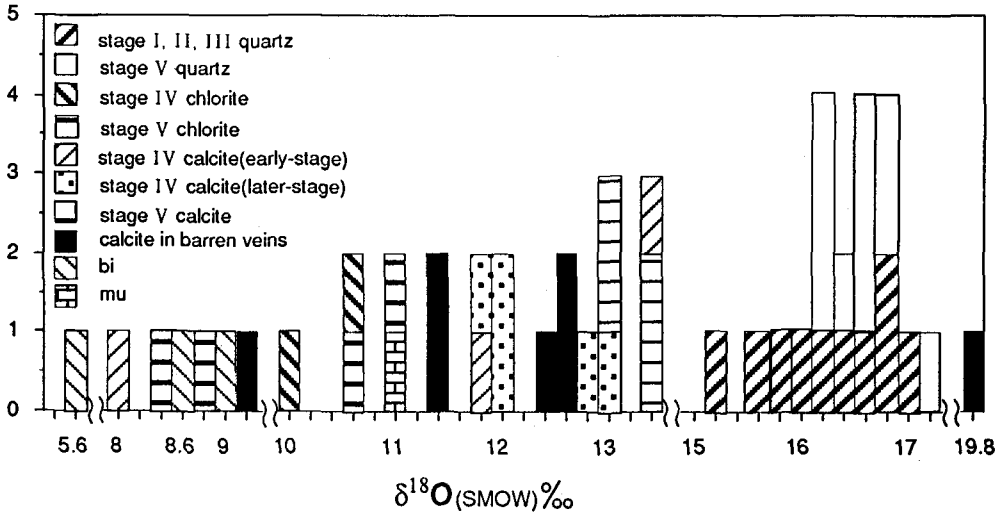

FIG. 7. Oxygen isotope composition of stages of quartz, calcite, chlorite, biotite and muscovite from veins and wallrock.

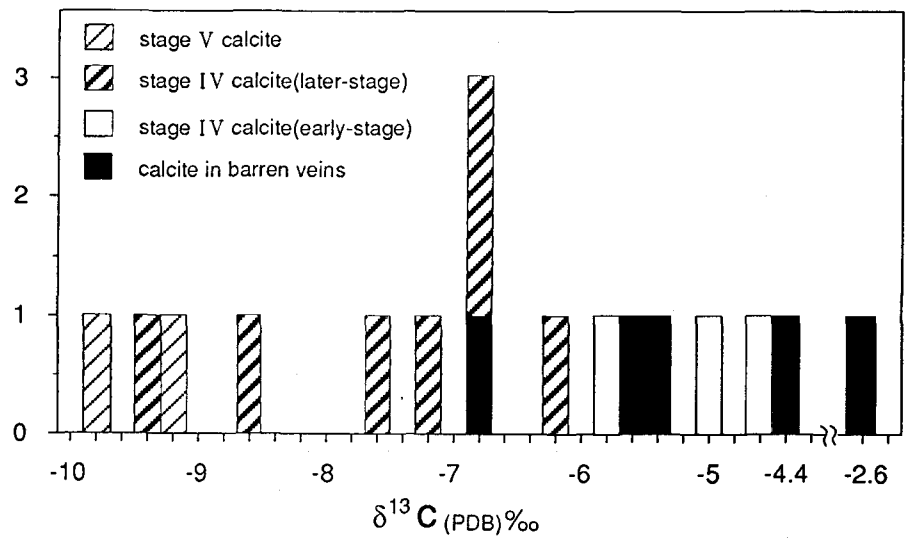

FIG. 8. Carbon isotope composition of different stages of vein calcite.

activity (Fig. 4). Calculated $\delta^{18}O$ compositon of fluid in equilibrum with the majority of calcite samples from the bedding-parallel veins ranges from 6.6 to 8.3‰. The results suggest that the fluid became progressively depleted in ^{18}O by about 2‰ during paragenetic stages III–V, when calcite precipitated, compared with the earlier mineralisation (stages I and II). This effect probably reflects an increase in the water-rock ratio during the final mineralising events, when the fluid was apparently dominated by meteoric water (Lu *et al.*, 1993, in press).

$\delta^{13}C$ composition ranges from −4.6‰ for fine-grained calcite deposited early in stage IV, to −9.7‰ for coarse-grained calcite developed late in stage IV. One possible reason for the systematic depletion in calcite $\delta^{13}C$ values in stage IV is the apparent decrease in the CH_4/CO_2 ratio accompanying the progressive increase in oxidation state of the mineralising fluids, assuming

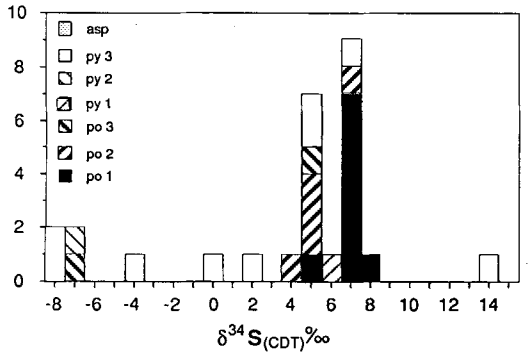

FIG. 9. Sulphur isotope composition of sulphides from veins and wallrock. Key: po1, py1–pyrrhotite, pyrite from bedding-parallel veins; po2, py2–pyrrhotite, pyrite disseminated in wallrocks; po3, py3–pyrrhotite and pyrite from late-stage fracture coatings and barren veins.

no significant change in the C-isotope composition during the deposition of stage IV calcite. Based on the isotopic enrichment factors at 300 °C (Bottinga, 1969), $H_2CO_{3(ap)}$ may be enriched in $\delta^{13}C$ by as much as 25.2‰ compared to CH_4(g, aq). This interpretation is supported by (*i*) the results of fluid inclusion gas phase analysis which show a remarkable decrease in CH_4/CO_2 ratios towards the later stages of fluid activity, and (*ii*) evidence from a change in mineral assemblages whereby pyrite becomes the dominant sulphide late in the stage IV event. An alternative possibility for ^{13}C depletion in stage IV calcite would involve an increasing contribution of a ^{13}C-depleted (mantle) C-source throughout this paragenetic stage.

In the mineral paragenesis, apart from sulphides, calcite is one of the most common minerals associated with gold. Therefore, conditions identified for calcite precipitation are likely to apply to gold deposition. Calculations based on the $\delta^{13}C$ distribution in calcite and the fO_2 values obtained from the composition of coexisting chlorite suggest that the most favourable redox environment for gold deposition is close to the CO_2–CH_4 stability boundary. This suggests that the phase transition involving these carbon species has an important role in gold precipitation.

$\delta^{34}S$ composition of eight out of the nine samples of pyrrhotite from the laminated veins lie in the very narrow range of 7.0–7.8‰. When pyrrhotite is the stable sulphide phase, H_2S is the dominant aqueous sulphur species and $\delta^{34}S_{H_2S(aq)}$ represents approximately the $\delta^{34}S_{fluid}$ of the ore-forming fluid (Ohmoto, 1972). Therefore, we can safely estimate that the $\delta^{34}S_{fluid}$ for the ore-forming fluid was close to 7.0‰ during stage III and IV, when most of the pyrrhotite precipitated.

In contrast with vein pyrrhotite, the $\delta^{34}S$ composition of pyrrhotite obtained from greywacke wallrock lies close to −4.9‰. Assuming a depositional temperature of 300 °C, a different S-source is implied for wallrock pyrrhotite ($\delta^{34}S_{fluid} \approx -4.9$‰) compared with the vein pyrrhotite.

The S-isotopic distribution in pyrite in barren quartz–calcite veins and from fracture planes in slate span a wide range ($\delta^{34}S = -8.5$ to 14.4‰). The wide variation in $\delta^{34}S$ values displayed by these pyrite samples is best explained by access to different sources of sulphur and local variations in fluid mixing ratios in the wallrocks. Fluid oxidation state is another factor which may have resulted in a wide range in pyrite $\delta^{34}S$ values, assuming a derivation from a S-source similar to either the vein or disseminated pyrrhotite and ignoring the minor influence of mineral–fluid isotopic fractionation. To account for $\delta^{34}S$ values in pyrite as low as −8.5‰, moderate oxidation of the fluid is implied. Pyrite deposited from such a fluid at 300 °C would be likely to demonstrate a range in $\delta^{34}S$ composition, because $\delta^{34}S_{H_2S(aq)}$ is very sensitive to slight changes in f_{O2} and pH under these conditions (Ohmoto and Rye, 1979).

Lead isotope study

To test the possible sources of lead in the auriferous veins, lead isotope determinations were undertaken on sulphides (pyrite, pyrrhotite and arsenopyrite) and gold, and compared with the lead isotope composition of a number of potential source rocks in the Hill End Trough. Measurements were made on a VG ISOMASS 54E thermal ionisation mass spectrometer as part of the cooperative Centre for Isotope Studies, North Ryde. All data are normalised to the NBS-SRM 981 common lead standard, using a correction factor of 0.08% per mass unit. Based on over 1500 analyses of this standard and replicate determinations of natural samples, the 2σ precision on the $^{206}Pb/^{204}Pb$ ratio is ± 0.1%.

Laminated bedding-parallel veins and leaders are characterised by two isotope populations in pyrite, galena, arsenopyrite and pyrrhotite, with $^{207}Pb/^{206}Pb$ ratios of about 0.862 (group 1) and 0.860 (group 2), distinguished by their 95% confidence ellipses in Fig. 10. It is noteworthy that five samples of gold taken from the Amalgamated and Mica veins and leaders to the Star of Hope vein, all belong to the population with lower $^{207}Pb/^{206}Pb$.

Differences between the two data groups may

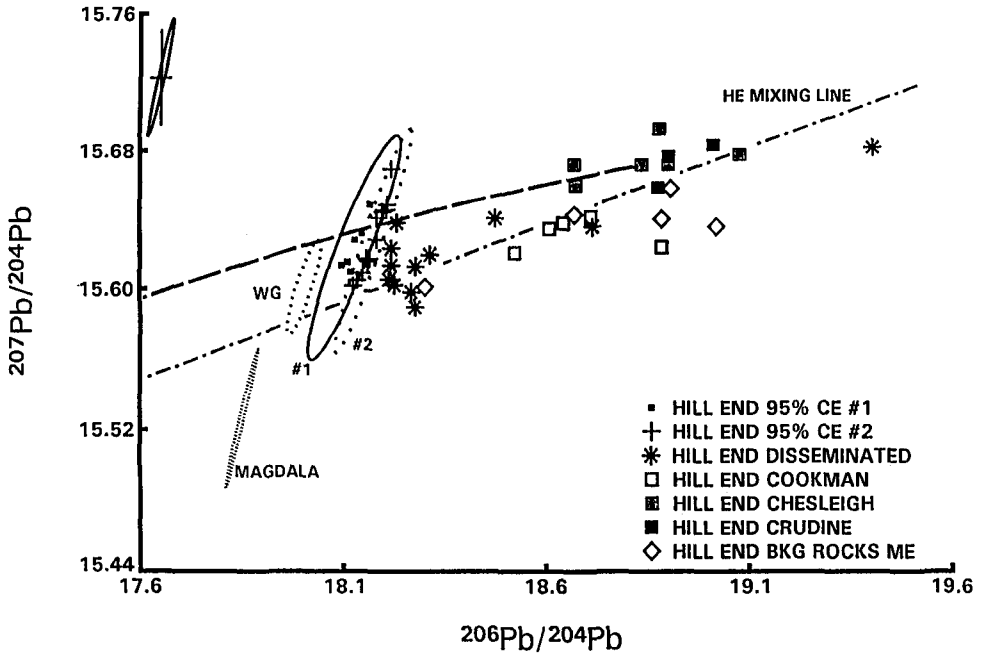

FIG. 10. $^{207}Pb/^{204}Pb$ *vs.* $^{206}Pb/^{204}Pb$ diagram for sulphides and gold from veins and wallrock. The 95% confidence ellipses (#1, #2) are given for two generations of vein minerals. Also shown are comparative data for the Wattle Gully (WG) and Magdala deposits and the suggested ore mixing line of disseminated sulphide and rock Pb from stratigraphic units in the Hill End Trough (Chesleigh and Cookman Formations, Crudine Group; Merrions Tuff). The growth curve for crustal lead (Cumming and Richards, 1975) is indicated by the dashed line.

relate to the economic importance of the sampled veins. High $^{207}Pb/^{206}Pb$ values are represented by pyrite and galena from barren leaders and some of the less important bedding-parallel veins in the mine area (Stevens and Mullocky veins), arsenopyrite in altered greywacke wallrock, and sulphides from minor laminated veins encountered in scout drilling several kilometres N of the Hill End field. An exception could be one sample of pyrite from the hangingwall of the Star of Hope vein.

Samples representing the population of low (group 2) $^{207}Pb/^{206}Pb$ values are all from highly productive veins in the center of the mining field. In structural order (Fig. 2) these include the Lady Belmore, Amalgamated, Phillipsons, Mica, Star of Peace and Star of Hope veins. The analysed minerals (pyrite, galena and gold) all come from veins on the E-dipping limb of the anticline.

The differences in isotopic composition for the vein system suggest that the fluids in each case were derived from different sources or were mobilised at different times. Either possibility is likely in a vein system established during a major deformation event. The recognition of stage V, coarse-grained calcite and abundant pyrite in samples representing the low $^{207}Pb/^{206}Pb$ population is good evidence of the late-stage nature of this gold bearing event.

The source of the gold is likely to be the Hill End trough-fill sequence. Isotopic data for high-lead samples of disseminated pyrrhotite, pyrite and arsenopyrite from the wallrocks have low $^{206}Pb/^{204}Pb$ values and lie close to the ellipse for the group 2 vein samples (Fig. 10). The disseminated sulphides, mine-area host-rocks and the ore samples define an array on a $^{207}Pb/^{204}Pb$ diagram which we interpret as a mixing line (Fig. 10). Local remobilisation of sulphide is not the main source of mineralisation, because wallrock sulphides have $^{206}Pb/^{204}Pb$ values higher than either of the two populations of vein minerals. Instead, we favour remobilisation and mixing of pre-existing rock sulphide and other background rock lead as the viable alternative. Variable mixing sources at slightly different times could account for the two isotope populations in the quartz veins. Relatively unform lead contents and isotopic compostions for the principal units of Silurian and Early Devonian age in the Hill End Trough (Chesleigh and Cookman Formations, Crudine Group; Fig. 10) allow these sedimentary units to

be the source of the metals. The similarity in lead content and isotopic composition of the younger Merrions Tuff permits this unit to be a partial melt of the underlying sediments.

Compared with similar turbidite-hosted gold deposits of the Victorian Ballarat-Bendigo Zone (Wattle Gully; Fig. 10), the Hill End goldfield samples have a lead isotope signature characterised by slightly higher $^{207}Pb/^{204}Pb$ and $^{206}Pb/^{204}Pb$, consistent with their derivation from a source with a higher crustal lead component. By contrast, a significant mantle lead component is evident in the data shown on Fig. 10 for the tholeiitic-volcanic hosted Magdala gold deposit of western Victoria.

Source of vein components and fluid evolution

The fluid source for quartz vein growth appears to be the underlying metasedimentary–metavolcanic sequence; an additional meteoric component is inferred for the late stages of mineralisation. The fluid composition, characterised by a variable content of N_2, CH_4 and CO_2, low salinity and low ionic content, appears to be typical of that from low-grade metamorphic rocks (Fyfe *et al.*, 1978; Kerrich, 1986) and is likely to represent fluid derived from dehydration reactions during prograde metamorphism of deforming crustal rocks (Goldfarb *et al.*, 1988). This is consistent with the O- and H-isotope composition of the ore-forming fluids and the mineralising temperatures derived from chlorite compositions and fluid inclusions.

The oxygen and hydrogen isotope data for the ore fluids do not support a direct magmatic component. Calculated $\delta^{18}O$ composition of the fluids associated with the deposition of quartz, chlorite, calcite, biotite, and muscovite (range: 6.6–11.0‰), δD values calculated from chlorite, biotite and muscovite (range: −35 to −98‰) and δD composition of the inclusion fluids (range: −53 to −77‰) generally occupy the region on a $\delta^{18}O$–δD distribution diagram which defines metamorphic water.

The sulphur isotopic composition of the ore-forming fluid at the time of sulphide deposition in the major laminated veins and leader veins ($\delta^{34}S_{\Sigma S}$ nearly 7‰) does not indicate a direct magmatic source of sulphur. These data, and widely ranging $\delta^{34}S$ values obtained from the wallrocks are best explained by leaching of rock sulphide from underlying metasedimentary or metavolcanic rocks.

Similar conclusions are drawn from the C-isotope data. $\delta^{13}C$ composition of the total carbon in the metamorphic fluid is about −5‰, calculated from the isotopic composition of calcite in syntectonic quartz–carbonate veins. The $\delta^{13}C$ composition of total carbon in the ore-forming fluid associated with gold deposition in the major veins bears the isotopic signature of carbon derived from the metamorphic rocks, mixed with an apparent deeper source of carbon, with a $\delta^{13}C$ value slightly lower than −7.2‰. This latter source of carbon is likely to have been derived by processes of decarbonation and degasification of carbon-bearing minerals and/or organic carbon during prograde metamorphism in the underlying volcano-sedimentary sequence (Lu *et al.*, 1993, in press).

By combining the stable isotope data, mineral chemistry and fluid inclusion evidence, a composite view of fluid evolution is obtained (Fig. 11). Barren fluids responsible for the precipitation of stage I and II quartz (Fig. 4) are identified by the presence of N_2 in the earliest fluid inclusions, CH_4 in later fluids and associated pyrrhotite, muscovite and chlorite (field 1 in Fig. 11). Gold, in

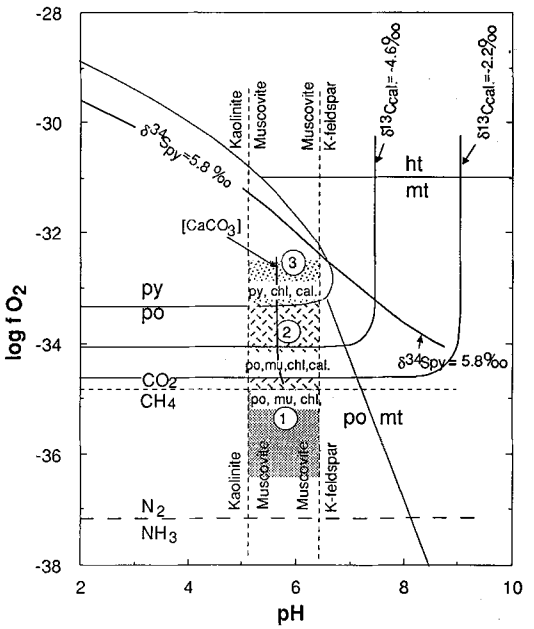

FIG. 11. Boundary f_{O2} and pH conditions at 300 °C, for fluid evolution in the Hill End vein systems, based on isotopic and mineralogical limits. Early mineralising fluids (field 1) are reducing, contain N_2 and are equilibrated with pyrrhotite, muscovite and chlorite. During the main episode (stage IV) of Au deposition (2), fluids contain abundant CH_4 and moderate CO_2 and are in equilibrium with pyrrhotite, muscovite, chlorite and calcite. In the last episode (stage V) of gold precipitation (3), as meteoric water enters the system, fluids are oxidising, pyrite, chlorite and calcite are stable phases and CO_2 is the dominant dissolved gas species.

equlibrium with pyrrhotite, muscovite, chlorite and calcite, precipitated from fluids in paragenetic stages III and IV, when CO_2 became a major species in the inclusion fluids, additional to CH_4 (field 2). Late-stage gold deposition during stage V, and the final episode of mineralisation are defined by oxidation of the ore fluid, following the entry of meteoric water to the system. In this last event, coexisting pyrite and calcite (+ chlorite) are the stable phases accompanying gold (field 3). Progressive depletion in $\delta^{34}S$ and $\delta^{13}C$, with each paragenetic stage of vein sulphide and calcite, parallels this evolutionary trend in the mineralising fluids (Fig. 11).

Mass-balance calculations by Seccombe and Hicks (1989), based on average rock compositions and likely fluid concentrations suggest that the gold content and other components of the veins can be adequately accounted for by mass-loss during cleavage formation in the underlying turbidite sequence. Source rocks enriched in gold relative to the turbidites may provide an additional or alternative source of that metal. Dismembered portions of the Ordovician island-arc volcanic sequences, which are known to be shoshonitic in affinity and basaltic to andesitic in composition, probably underlie the Hill End Trough, and could play an important role in sulphur and metal generation.

Transport of gold in the low salinity, reduced metamorphic fluid would take place through the formation of a gold thio-complex (Seward, 1984). Fluid migration was controlled by bedding planes initially, and to a lesser extent, by cleavage and fracturing later in the deformation event. Regional structure, especially culminations of anticlinal crests, appears important in focussing the flow of fluids and promotes ponding beneath less permeable greywackes in the hostrock sequence. Sandstone and greywacke beds have been identified elsewhere as low permeability rock units that may have acted as structural traps in anticlinal hinge zones developed in turbidite sequences (Nova Scotia: Mawer, 1986; Central Victoria: Cox *et al.*, 1991). Deposition of gold at Hill End occurred in apparent response to gold thio-complex destabilisation, either through H_2S loss from the fluid system, or a change in the redox environment (Brand *et al.*, 1989; Shepherd *et al.*, 1991). In the early stages of mineralisation, in the presence of CH_4 (and/or N_2) in the fluid phase, phase separation, possibly resulting from transient pressure loss during vein opening, will induce a drop in a_{H_2S} of the aqueous, gold transporting fluid. Sulphidation reactions in the wallrocks or deposition of sulphide minerals in the veins also provide an effective mechanism for gold precipitation by depletion of the H_2S ligand in the fluid. Lastly, because the stability of the $Au(HS)_2^-$ complex is redox sensitive, loss of H_2S through oxidation could lead to Au precipitation (Brand *et al.*, 1989). This may be an important factor towards the later stages of mineralisation, when changes in $\delta^{34}S_{fluid}$ appear to result from oxidation of the ore fluid.

Acknowledgements

We would like to thank the management and staff of Silver Orchid Limited, especially Robert Cleaver, Barry and Hilary Montgomery and Alan Dennington for hospitality and support during mapping and sampling at Hill End. W. Crebert, J. Crawford and H. Nesmithruming are thanked for the drafting and photography. The help given by Dr Terry Mernagh, Bureau of Mineral Resources, Canberra in providing laser Raman analyses of fluid inclusions is very much appreciated. The Centre for Isotope Studies is a cooperative venture between the Division of Exploration Geoscience, CSIRO, North Ryde and a consortium of nine Universities, with financial assistance from the Australian Research Council. The consortium universities are: James Cook, Macquarie, Newcastle, New England, New South Wales, Queensland, Technology Sydney, Sydney and Wollongong. Financial assistance for this research was provided by grants from the University of Newcastle, CSIRO and the Australian government through the International Geological Correlation Program.

References

Bigeleisen, J., Pearlman, M. L., and Prosser, H. C. (1952) Conversion of hydrogenic materials to hydrogen for isotopic analysis. *Analyt. Chem.*, **24**, 1356–7.

Bottinga, Y. (1969) Calculation of fractionation factors for carbon and hydrogen isotope exchange in the system calcite–CO_2–graphite–methane and water vapor. *Geochim. Cosmochim. Acta*, **33**, 49–64.

Bowers, T. S. and Helgeson, H. C. (1983) Calculations of the thermodynamic and geochemical consequences of nonideal mixing in the system H_2O–CO_2–NaCl on phase relations in geological systems: Equation of state for H_2O–CO_2–NaCl fluids at high pressures and temperatures. Ibid. **47**, 1247–75.

Brand, N. W., Bottrell, S. H., and Miller, M. F. (1989) Concentrations of reduced sulphur in inclusion fluids associated with black shale hosted quartz vein gold deposits: implications for mechanisms of transport and deposition of gold and a possible exploration tool. *Appl. Geochem.*, **4**, 483–91.

Clayton, R. N. and Mayeda, T. K. (1963) The use of bromine pentafluoride in the extraction of oxygen from oxides and silicates for isotopic analysis. *Geochim. Cosmochim. Acta*, **27**, 43–52.

Clayton, R. N., O'Neil, J. R., and Mayeda, T. K. (1972) Oxygen isotope exchange between quartz and water. *J. Geophys. Res.*, **77**, 3057–67.

Collins, A. G. (1971) *The morphology of slaty cleavage*

in the Hill End Trough. PhD thesis (unpubl.) Univ. Sydney, Australia.

Cox, S. F., Wall, V. J., Etheridge, M. A., and Potter, T. F. (1991) Deformational and metamorphic processes in the formation of mesothermal vein-hosted gold deposits—examples from the Lachlan Fold Belt in central Victoria, Australia. *Ore Geol. Rev.*, **6**, 391–423.

Cumming, G. L. and Richards, J. R. (1975) Ore lead isotope ratios in a continuously changing Earth. *Earth Planet. Sci. Lett.*, **28**, 155–71.

Fyfe, W. S., Price, N. J., and Thompson, A. B. (1978) *Fluids in the Earth's Crust.* Elsevier, Amsterdam, 383pp.

Goldfarb, R. J., Leach, D. L., Pickthorn, W. J., and Paterson, C. J. (1988) Origin of lode-gold deposits of the Juneau gold belt, southeastern Alaska. *Geology*, **16**, 440–3.

Hicks, M. N. (1977) *The geology and quartz vein genesis of the Hawkins Hill area, Hill end, New South Wales.* BSc.(hons.) thesis (unpubl.) Univ. Newcastle, Australia.

Ho, S. E. (1987) Fluid inclusions: their potential as an exploration tool for Archaean gold deposits. In *Recent Advances in Understanding Precambrian Gold Deposits* (Ho, S. E. and Groves, D. I., eds.). Geol. Dept. Univ. Western Australia, **11**, 239–63.

Kerrich, R. (1986) Fluid infiltration into fault zones: Chemical, isotopic and mechanical effects. *Pure Appl. Geophys.*, **124**, 225–68.

Lu, J. and Seccombe, P. K. (1993, *in press*) Fluid evolution in a slate-belt gold deposit: A fluid inclusion study of the Hill End goldfield, NSW, Australia. *Mineral. Deposita.*

——Seccombe, P. K., Walshe, J. L., Gulson, B. L., and Mizon, K. J. (1993, in press) Source of components and conditions of mineralisation in the Hill End goldfield, NSW: Evidence from S, C, O, H and Pb isotopes, fluid inclusions and the composition of chlorite. *Econ. Geol.*

McCrea, J. M. (1950) On the isotope chemistry of carbonates and paleotemperature scale. *J. Chem. Phys.*, **18**, 849–57.

Mawer, C. K. (1986) The bedding-concordant gold–quartz veins of the Meguma Group, Nova Scotia. In *Turbidite-hosted Gold Deposits* (Keppie, J. D. *et al.*, eds.). Geol. Assoc. Canada Special Paper, **32**, 135–48.

Offler, R. and Prendergast, E. (1985) Significance of illite crystallinity and b_0 values of K-white mica in low grade metamorphic rocks, North Hill End Synclinorium, New South Wales. *Mineral. Mag.*, **49**, 357–64.

Ohmoto, H. (1972) Systematics of sulfur and carbon isotopes in hydrothermal ore deposits. *Econ. Geol.*, **67**, 551–78.

——and Rye, R. O. (1979) Isotopes of sulfur and carbon. In *Geochemistry of Hydrothermal Ore Deposits* (Barnes, H. L., ed.). Wiley Interscience, New York, 509–67.

O'Neil, J. R. and Taylor, Jr., H. P. (1969) Oxygen isotope equilibrium between muscovite and water. *J. Geophys. Res.*, **74**, 6012–22.

Powell, C. McA. and Edgecombe, D. R. (1978) Mid-Devonian movements in the north eastern Lachlan Fold Belt. *J. Geol. Soc. Austral.*, **25**, 165–84.

——Edgecombe, D. R., Henry, N. M., and Jones, J. G. (1976) Timing of the regional deformation of the Hill End Trough: A reassessment. Ibid., **23**, 407–21.

Powell, R., Will, T. M., and Phillips, G. N. (1991) Metamorphism in Archaean greenstone belts: calculated fluid compositions for gold mineralization. *J. Metam. Geol.*, **9**, 141–50.

Ramsay, J. G. (1980) The crack–seal mechanism of rock deformation. *Nature*, **284**, 135–9.

Roedder, E. (1984) *Fluid Inclusions.* Reviews in Mineralogy, **12**, Mineralogical Society of America, Washington, 644pp.

Robinson, B. W. and Kusakabe, M. (1975) Quantitative preparation of sulfur dioxide for $^{34}S/^{32}S$ analyses form sulfides by combustion with cuprous oxide. *Anal. Chem.*, **47**, 1179–81.

Sakai, H. and Tsutsumi, M. (1978) D/H fractionation factors between serpentine and water at 100 °C to 500 °C and 200 bar water pressure and the D/H ratios of natural serpentines. *Earth Planet. Sci. Lett.*, **40**, 231–42.

Seccombe, P. K. and Hicks, M. N. (1989) The Hill End goldfield, NSW, Australia—Early metamorphic deposition of auriferous quartz veins. *Mineral. Petrol.*, **40**, 257–73.

Seward, T. M. (1984) The transport and deposition of gold in hydrothermal systems. In *Gold '82: The Geology, Geochemistry and Genesis of Gold Deposits* (Foster, R. P., ed.). A. A. Balkema, Rotterdam, 165–81.

Shepherd, T. J., Bottrell, S. H. and Miller, M. F. (1991) Fluid inclusion volatiles as an exploration guide to black shale hosted gold deposits, Dolgellau gold belt, North Wales, UK. *J. Geochem. Explor.*, **42.** 5–24.

Sterner, S. M. and Bodnar, R. J. (1989) Synthetic fluid inclusions–VII. Re-equilibration of fluid inclusions in quartz during laboratory-simulated metamorphic burial and uplift. *J. Met. Geol.*, **7**, 243–60.

Stevens, B. P. J. (1974) Hill End synclinorial zone. In *The Mineral Deposits of New South Wales* (Markham, N. L. and Basden, H., eds.). Geol. Surv. New South Wales, Dept. Mines, Sydney, 276–93.

Suzuoki, T. and Epstein, S. (1976) Hydrogen isotope fractionation between OH-bearing minerals and water. *Geochim. Cosmochim. Acta*, **40**, 1229–40.

Taylor, Jr., H. P. (1979) Oxygen and hydrogen isotope relationships in hydrothermal ore deposits. In *Geochemistry of Hydrothermal Ore Deposits* (Barnes, H. L., ed.). Wiley Interscience, New York, 236–77.

Walshe, J. L. (1986) A six-component chlorite solid solution model and the conditions of chlorite formation in hydrothermal and geothermal systems. *Econ. Geol.*, **81**, 681–703.

Windh, J. (1993, in press) Saddle-reef and related gold mineralization, Hill End Goldfield, Australia: Evolution of an auriferous vein system during progresive deformation. Ibid.

[*Manuscript received 13 September 1992: revised 5 March 1993*]